

Fluorescence laser scanner for in-line inspection of functional coatings in metal processing industries

Philipp Holz*^a, Albrecht Brandenburg^a

^a Fraunhofer Institute for Physical Measurement Techniques IPM,
Heidenhofstrasse 8, 79110 Freiburg, Germany

ABSTRACT

Metal processing industries utilize two types of functional coatings. Conversion coatings, based on Zirconium and/or Titanium, generate corrosion resistance and paint adhesion for aluminum surfaces. Another type of functional coatings are lubricants based on mineral oil, which act as corrosion protection as well as drawing and punching oil. Efficient process development and control requires the monitoring of the thickness of these functional coatings.

In this article, we present a new optical setup, which uses a rotating polygon-scanning mirror in combination with laser-induced fluorescence to monitor the spatial distribution of lubricants and conversion coatings on metal sheets. In the presented setup, the beam of a 405 nm diode laser excites auto-fluorescence of the organic molecules inside the functional coatings. By using a fast rotating scanner mirror combined with a fast analogue digital conversion, the presented setup reaches data rates of 400 lines/s consisting of 1000 data points each. Installing the scanner system at a distance of 1200 mm above the metal sheets, realizes a field of view of 2200 mm. At strip speeds of 2 m/s, the distance between two scanner lines on the surface to be investigated is 5 mm.

In addition to the description of the optical system, we present different approaches for the calibration of systems for in-line fluorescence measurements. For the calibration of lubricant layers in the range down to one micrometer, the reference samples are weighted. To evaluate the limit of detection of the system we use a multiphase carbon analyzer. We show the calibration results for different lubricants and metal materials with different surface textures typically used in car body manufacturing.

Keywords: Measurement and analysis of corrosion protection, Measurement and analysis of lubrication, Calibration of fluorescence laser scanner, Quantitative fluorescence measurement, Fluorescence imaging

1. INTRODUCTION

Metal processing industries utilize two types of functional coatings. Conversion coatings, based on Zirconium and/or Titanium, generate corrosion resistance and paint adhesion for e.g. aluminum surfaces. Many of these conversion coatings contain organic additives. Another type of functional coatings are lubricants based on mineral oil, which act as corrosion protection as well as drawing and punching oil. As in car body part production process windows and lot sizes decrease, current research in this area focuses on the identification of influential factors and existing correlations in the overall production process¹. One promising method is the use of data mining to achieve a data driven process control in the manufacturing of car body parts^{1,2}. Despite others, one important variable influencing the quality of the car body part production process is the friction between stamping tool and metal surface³. Therefore the lubricant level on the metal surface is considered in all models for the data driven process control and optimization^{1,2,4}.

Currently there is no method for in-line measurements of conversion coatings available in industry. Measurement systems for the determination of lubricant layer thickness are based either on infrared spectroscopy or on fluorescence spectroscopy^{5,6,7,8}. The width of metal coils in industrial applications is up to two meters. Figure 1 shows the working principle of current sensors for inline-measurements of lubricant layers on metal coils. To record information on the lubricant distribution, the sensor heads of current sensors need to move along the object on a linear axis^{5,6}. Due to the limited traversing speed typically below 1 m/s orthogonal to the movement of the metal strips, these systems cannot analyze the complete metal surface at high strip speeds.

*philipp.holz@ipm.fraunhofer.de; phone +49 761 8857-380; fax +49 761 8857-224; www.ipm.fraunhofer.de

At strip speeds of 2 m/s at press plants, a strip width of 2 m and a traversing speed of 1 m/s, the distance between two measurement points in feed direction is up to 8 meter. For this reason, systems mounted on traversing units are not capable of measuring the lubricant distribution on the complete surface of metal strips.

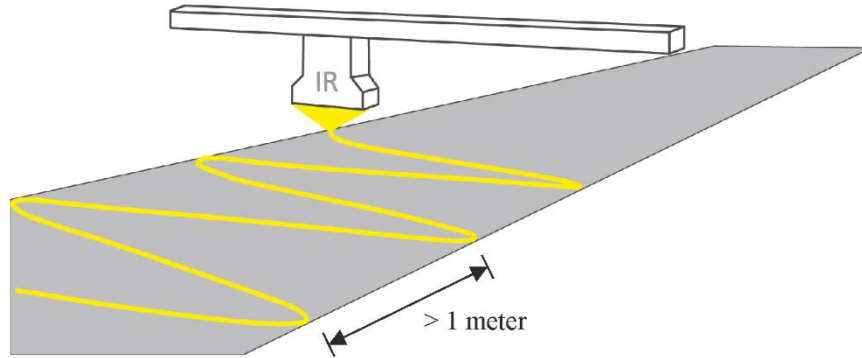


Figure 1. To record information of the lubricant distribution, the sensor heads of current sensors need to move along the object on a linear axis. Therefore, the spatial resolution of these systems is insufficient at strip speeds, which are typically more than 1 m/s.

Laser scanning or camera systems can be used to overcome this limitation of spatial resolution. In literature camera systems for fluorescence imaging are described for example for the measurement of the oil-film thicknesses in a piston-ring area^{9,10}. The field of view of these setups are only of some square millimeters and dyes have to be used to enhance the fluorescence signals. A combined setup with scanning mirrors and laser induced fluorescence is described for systems used to monitor oil spills on the sea surface^{11,12}. These systems are installed at airplanes. Components used in these setups are fairly expensive and not suitable for industrial applications. In previous work, we presented a 2D laser scanner. This lab system allows the acquisition of fluorescence images of an area of 300 x 300 mm² at a spatial resolution of 1.1 mm in less than 20 seconds¹³.

Typical metal blanks used in car body production have a width of up to 2.2 meter. To allow the installation of the new measurement system in existing press plants, the maximum height of the complete optical setup should not be larger than 1.6 meter. Aim of the research leading to this paper was to develop an in-line measurement system that meets the requirements on spatial resolution, speed and sensitivity to monitor the thickness of functional coatings in industrial forming processes.

2. EXPERIMENTAL

To meet the described requirements on spatial resolution and film thickness sensitivity the developed system uses a polygon-scanning mirror in combination with laser-induced fluorescence in order to monitor the spatial distribution of lubricants on moving metal strips. For the characterization of the developed system, custom designed samples are used.

2.1 Calibration for quantitative measurements

The dependence of the fluorescence signal on film thicknesses is well described in literature¹⁴. According to Beer-Lambert law incident light with the power P_0 is attenuated as a function the thickness d of an absorbing layer and the attenuation coefficient α of the medium at the wavelength λ_{ex} of the incident light. The power of the absorbed light P_{abs} over a certain optical path length d is described by

$$P_{abs}(d) = P_0(1 - e^{-\alpha d}). \quad (1)$$

For low film thicknesses and/or low absorbance values according to the condition $\alpha d \ll 1$ the first term of the Taylor series can be used as valid approximation for the exponential term in equation 1.

$$e^{-\alpha d} \approx 1 - \alpha d. \quad (2)$$

The quantum yield Q is defined as the ratio of the number of emitted photons to the number of absorbed photons. Therefore the power of the fluorescence emission P_f can be described as:

$$P_f(d) = Q \frac{\lambda_{ex}}{\lambda_{em}} \cdot P_{abs}(d), \quad (3)$$

with the ratio between λ_{ex} and λ_{em} describing the loss of power due to the stokes-shift between the excitation and emission wavelength. Using equation 1 to 3 the fluorescence emission for low absorbance values αd can thus be written as

$$P_f(d) = Q \frac{\lambda_{ex}}{\lambda_{em}} P_0 \alpha d. \quad (4)$$

In practice the portion of the fluorescence emission which reaches the detector aperture depends on a on the sensor geometry, the properties of the optical components and the distance l between fluorescence emission and detector aperture. The spectral response of the detector further influences the detector signal U_d . These system-specific properties can be described in a proportional factor k

$$U_d(d) \approx k \frac{1}{l^2} P_f(d) \quad (5)$$

For calibration, we prepare lubricant layers with an initially unknown thickness. Subsequent we determine the average layer thickness of the prepared layer either with a high-resolution balance or by a multiphase carbon analyzer. The then known samples are subsequently analyzed with the laser scanner.

2.2 Sensor design

We used two types of fluorescence laser scanner systems for the work presented in this paper. A previously presented lab setup was used to analyze the emission characteristic of fluorescent layers on different surfaces. We used the same lab setup to show the possibility to calibrate fluorescence systems using a multiphase carbon analyzer as reference measurement system.

The major work presented in this paper was the development of a laser scanner for the in-line monitoring of functional coatings on metal samples directly in the production environment.

Lab setup: 2D scanner system

Figure 2 shows the 2D scanner system used in this publication. As shown in Figure 2a, the optical setup is installed on top of a sample chamber to ensure laser safety. In order to use a robust, durable and relatively cheap laser and to achieve a good limit of detection we use a 405 nm diode laser module with 300 mW optical power for the excitation of the samples. A two-axis galvanometer scanner deflects the beam of the excitation laser to scan the bottom of the sample chamber. A

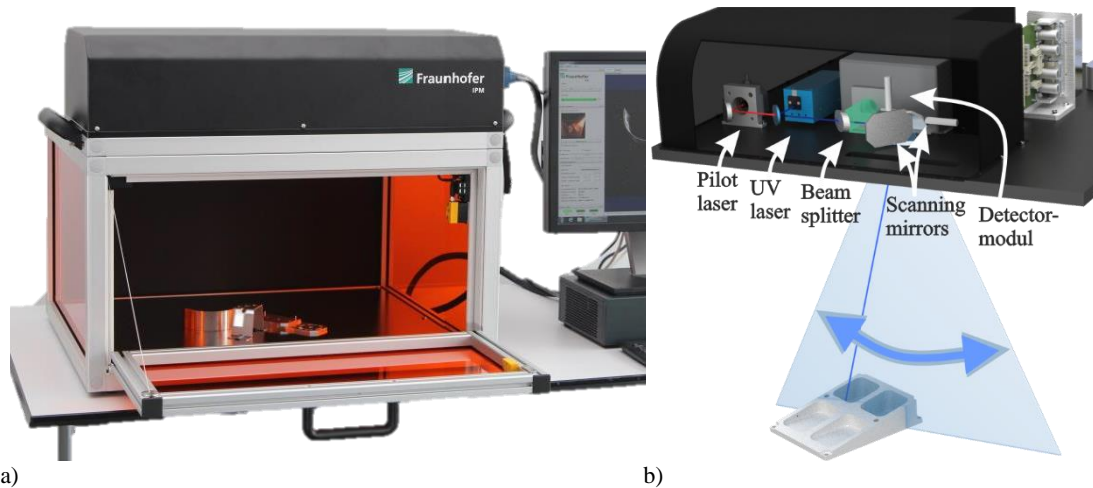


Figure 2. Concept of the previously presented lab system¹³. As shown in the left picture (a) the optical setup is installed on top of a sample chamber. The right figure (b) shows details of the optical setup.

The excitation laser induces fluorescence locally on the sample inserted into the sample chamber. A portion of the emitted fluorescence light is collected back by the scanning mirrors. For a sensitive detection, a large diameter of the scanning mirrors of one inch is chosen. A beam splitter in combination with chromatic filters guides the fluorescence light on the detector. We use a photomultiplier to detect the fluorescence light in the spectral range of 420 to 520 nm. In this lab system, we use a PC equipped with a PCI Express I/O card for data acquisition as well as control of the scanning mirrors and photomultiplier amplification. Custom-made software generates all control signals and visualizes the fluorescence signals as two-dimensional image.

The scanning mirrors allow the deflection of the laser beams of an angle of $\pm 20^\circ$. As the optical system is installed 300 mm above the bottom of the sample chamber the field of view of the presented system is $300 \times 300 \text{ mm}^2$. As previously presented, the optical resolution of this lab system is better than $400 \mu\text{m}^{13}$. This means that gaps between lubricant droplets down to a width of $200 \mu\text{m}$ can still be visualized. The limit of detection of this lab system was determined to be better 0.05 g/m^2 for certified lubricant BAM K-009¹³. Due to the use of a nearly collimated laser beam, the depth of focus of the system is several centimeters. This allows the analysis of three dimensional freeform objects as well as tilted samples.

In-line system: 1D scanner system

Figure 3 shows the new optical system presented in this paper. To achieve the required spatial resolution at strip speeds up to 2 m/s on one-hand side scan-rates of several hundred lines per second are required. Experiments done with the lab setup showed, that on the other hand an aperture of the detector optics of at least one inch is required to secure a sufficient limit of detection. Due to the oscillating principle, two-axis galvanometer scanners with one inch aperture are limited to maximum 30 lines per second. Therefore, we use a rotating polygon mirror in the presented in-line setup.

To fulfill the requirement on installation space in existing press plants, either several optical units can be placed next to each other or the optical unit must have a large field of view. As shown in Figure 3 we use a symmetrical two-channel setup to realize an angular scan field of 80° . Figure 4 shows the installation drawing for the presented scanner system. As shown in Figure 4 the required field of view of 2.2 m is reached if the distance between bottom of the optical unit and the metal blank is $l_\perp = 1.2$ meters. As the height of the housing is 32 cm, the total installation space is 1.52 m.

The optical setup of both channels is identical. For excitation of the fluorescence, we use a 405 nm diode laser module with 300 mW optical power. The polygon mirror deflects the excitation lasers towards the sample. The same polygon mirror collects a portion of the fluorescence light emitted on the sample surface. Similar to the previously described lab setup we use a chromatic beam splitter in combination with optical filters to direct the fluorescence light on the detectors. We use a photomultiplier on each channel to detect the fluorescence signal between 420 and 520 nm.

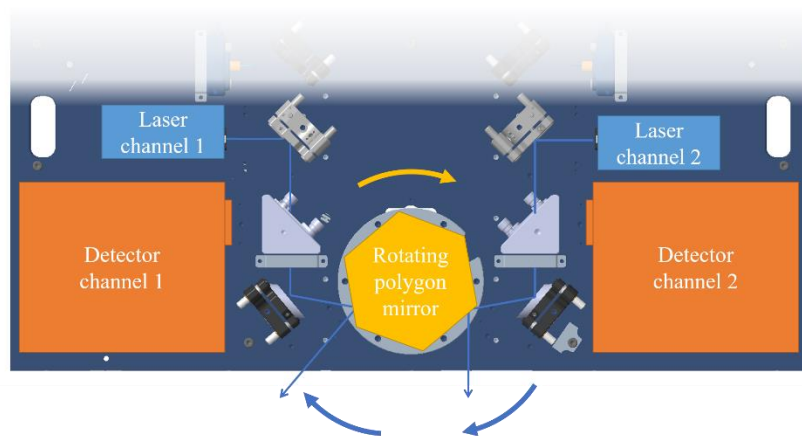


Figure 3. Concept of the new optical in-line system. A rotating polygon mirror deflects the excitation lasers towards the sample. The same polygon mirror collects a portion of the fluorescence light emitted on the sample surface.

All optical components are mounted on one side of an aluminum board. On the back of the same board, all electrical components are installed. A USB-based data acquisition (DAQ) board samples the analog photomultiplier signal directly inside the optical unit. The same DAQ-board provides the control voltage for the amplification of the photomultiplier.

We use a 100 W brushless DC motor for rotating the polygon mirror. This motor allows a speed of 4000 rpm. Considering the six-faceted polygon mirror, this leads to a scan rate of 400 lines per second.

USB signals from the DAQ-board, from the laser modules as well as from the motor driver are converted to gigabit Ethernet signals inside the sensors housing to avoid electrical interferences at production environments.

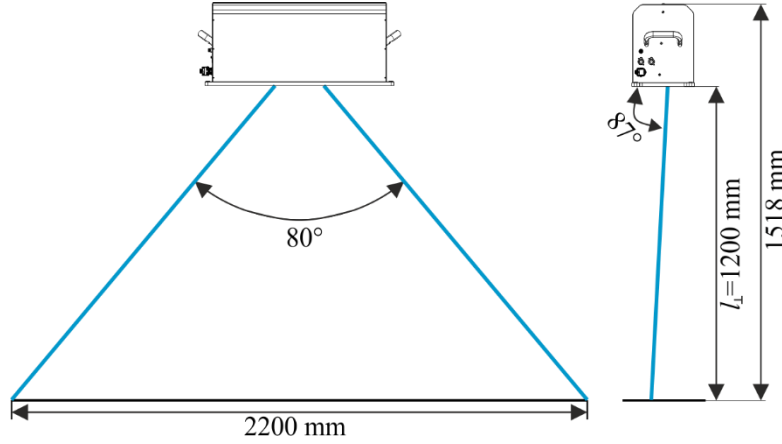


Figure 4. Installation drawing showing the front and side view of the scanner system. The angular scan field of the presented fluorescence laser scanner is 80° degrees. Therefore, installing the scanner system at a distance of $l_L = 1.2$ m above the sample, realizes a field of view of 2.2 m.

2.3 Reference target for sensor normalization

As described in equation 5 the detector signal U_d depends on system-specific properties described by the proportional factor k . To generate system-independent results we normalize all detector signals $U_{d,sa}$ of the sample on the signal $U_{d,ref}$ detected when analyzing a reference target. Due to this normalization the system-specific proportional factor k is mathematically canceled which leads to the system-independent normalized fluorescence response F_n . Applied on equation 5 this normalized fluorescence response F_n is described by the relation of the fluorescence emission $P_{f,sa}$ of the sample and the fluorescence emission of the reference target $P_{f,ref}$ by

$$F_n(d) \approx \frac{U_{d,sa}(d)}{U_{d,ref}} = \frac{P_{f,sa}(d)}{P_{f,ref}}. \quad (6)$$

Therefore, the normalized fluorescence response F_n describes the emission of fluorescent layers as a function of the layer thickness independent of the properties of the optical measurement system.

As reference target we use a solid target made of Spectralon® fluorescence material (Labsphere Type 461: USFS-461-020; 2"). This fluorescence standard has the shape of a disc with a diameter of 2 inches. According to Labsphere the fluoropolymer material Spectralon® is used as a matrix for inorganic fluorophores which are photochemically stable when compared to their organic counterparts¹⁵. Due to the light scattering surface properties the targets light absorbance is independent of the angle of incidence. Therefore, the fluorescence emission of the target is independent of the variation of the optical setup of the fluorescence excitation in different fluorescence measurement systems.

2.4 Sample preparation

For sample preparation, sheets of the size of 80 x 80 mm² are cut out of different metal samples. Before the coating, all samples are cleaned using Heptane.

Figure 5 shows microscope images of the surface texture of sample substrates used for calibration. The images were acquired with a 3D confocal laser scanning microscope (Keyence, VK 9700). The metal types shown in Figure 5 are typically used in car body manufacturing. Metal blanks for automotive car bodies are often textured by electric

discharged texturing (EDT) to improve the forming behavior due to better friction behavior.¹⁶ The so-called precision texturing (Pretex®) is a roller texturizing process, which according to manufacturer Salzgitter Flachstahl ensures uniform, defined roughness values for steel sheet surfaces. Surface pockets created by the texturing serve as a lubricant reservoirs and improve the friction and lubrication conditions during deformation¹⁷.

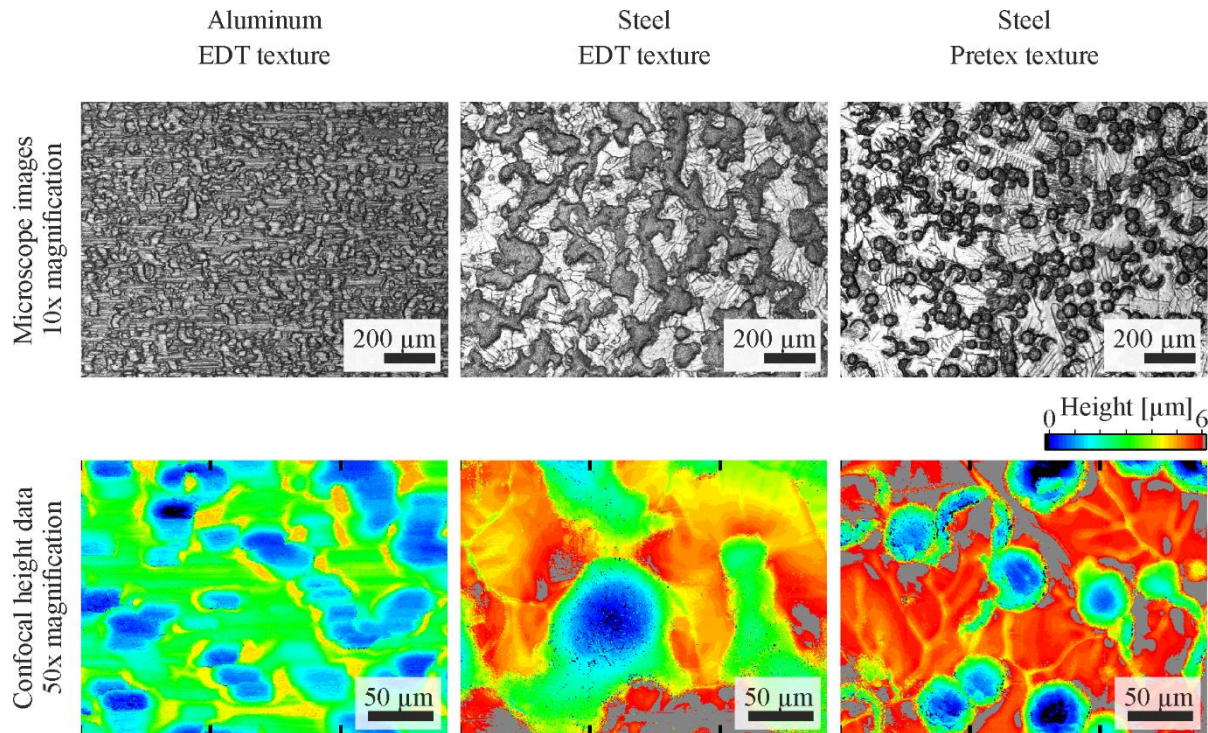


Figure 5. Microscope images of the surface textures of the metal samples used for the presented work. The height data was acquired using a 3D confocal laser-scanning microscope.

For the application of homogeneous lubricant layers, we use a rubber wallpaper roll. To prevent the absorption of lubricant by the rubber the rubber roll is covered with aluminum foil.

A spray unit is used to apply oil droplets on different substrates. To adjust the oil density on the surface the substrate is moved for several times at different speeds through the oil dust.

For the calibration of lubricant layers higher than 0.2 g/m^2 we use a high-resolution balance (Sartorius, MSE225P-100-DU) as reference. The weight of all metal samples is determined before and after coating using the balance. The average area density of the lubricant layer is then calculated by dividing the weight gain caused by the lubricant by the area of the metal sample. For the work presented in this paper we prepared lubricant layers in the range from 0.2 to 2 g/m^2 with the forming oil KTL N 16 (Zeller+Gmellin) as well as a lubricant for corrosion protections RP 4107 S (Fuchs).

For the calibration of thin lubricant layers as well as to determine the limit of detection of the developed measurement systems, we use a multiphase carbon analyzer (LECO Corporation, RC612) as reference. In contrast to the gravimetric calibration, this method destroys the samples during the reference measurement. Therefore, we acquire fluorescence images of the samples directly after preparation. Afterwards the metal sheets are cut into small slices of the size of ca. $1 \times 2 \text{ cm}^2$. The multiphase carbon analyzer combusts the lubricant on the samples surface at temperatures up to 750°C .¹⁸ Since the samples are combusted in a pure oxygen stream, carbon released by the lubricant reacts to carbon dioxide. The total amount carbon dioxide is analyzed using a calibrated infrared detector. For calibration, we correlate the amount of surface carbon with the average fluorescence signal. It has to be considered that the result of the multiphase carbon analysis includes carbon combusted on both sides of the sample surface. Therefore, either fluorescence images of both sides of the samples must be acquired or the bottom side of the sample has to be free of any organic residuals. For the work presented in this paper, we prepared thin layers of a rolling oil on clean copper blanks using a rubber roll covered with aluminum foil.

3. RESULTS

3.1 Gravimetric Calibration for quantitative measurements of lubricants

Figure 6 exemplarily shows fluorescence images of four samples used for the calibration. The fluorescence images show EDT textured aluminum samples coated with the forming oil KTL N 16. Sample 1 and 4 were coated with 0.6 g/m^2 , sample 3 with 1.2 g/m^2 and sample 2 with 1.7 g/m^2 . The images presented in Figure 6a were acquired with the lab system described in section 2.2. The difference between the preparation of the lubricant layers as closed film by rolling or single droplets by spraying the lubricant is clearly visible. Whereas rolling leads to closed lubricant layers, single lubricant droplets are generated on the sample surface by spraying. Figure 6b shows the fluorescence images of the same samples acquired with the newly developed in-line System.

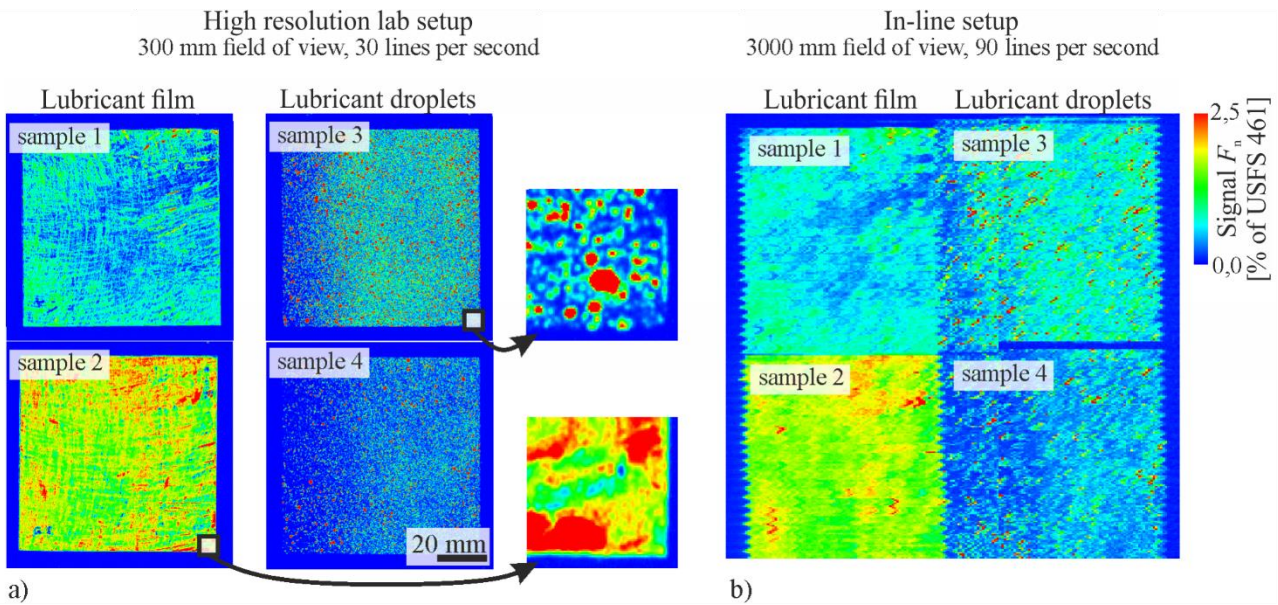


Figure 6. Fluorescence images of four samples used for the calibration. The images of the same samples were acquired by the high-resolution lab setup (a) as well as by the new in-line setup (b). The difference between the preparation of the lubricant layers, as closed film by rolling and single droplets by spraying the lubricant, is clearly visible in the high-resolution images.

For the calibration, the average fluorescence signal of each sample is analyzed. For example, the average signal of sample 1 and 4 is nearly identical, despite the different lubricant distribution visible in the false color representation shown in Figure 6a. Figure 7 shows the fluorescence response F_n acquired with the lab system as function of the gravimetrically determined area density of the applied lubricant layers. For the experiments leading to the results presented in Figure 7 the lubricant layers were prepared by rolling. As defined in equation 6, all fluorescence emissions $P_{f,sa}$ are normalized to the fluorescence emission $P_{f,ref}$ of the reference target USFS-461.

As described by equation 4 and 6, the results presented in Figure 7 show a linear relation between the detected fluorescence signal F_n and the thickness of the lubricant layer.

Figure 7a) compares the results of the calibration for the forming oil KTL N 16 on three different surfaces. These results indicate that both the surface material as well as the surface texture influence the fluorescence response per layer thickness. Lubricant layers coated on pretex textured steel emit the strongest fluorescence response. The fluorescence response of lubricant layers coated on EDT textured steel is 40 percent less compared to pretex textured steel. Lubricant layers applied on EDT textured aluminum surfaces show a 15 percent weaker fluorescence response per layer thickness compared to layers coated on pretex textured steel.

Figure 7b) visualizes the calibration for the lubricant for corrosion protection RP 4107 S applied on steel samples with a EDT textured surface. For this lubricant, the fluorescence signal per area density of lubricant is more than one order of magnitude lower than for the lubricant KTL N 16. This deviation in the fluorescence response can be explained by different material coefficients for the absorbance value α and the quantum yield Q for both lubricants.

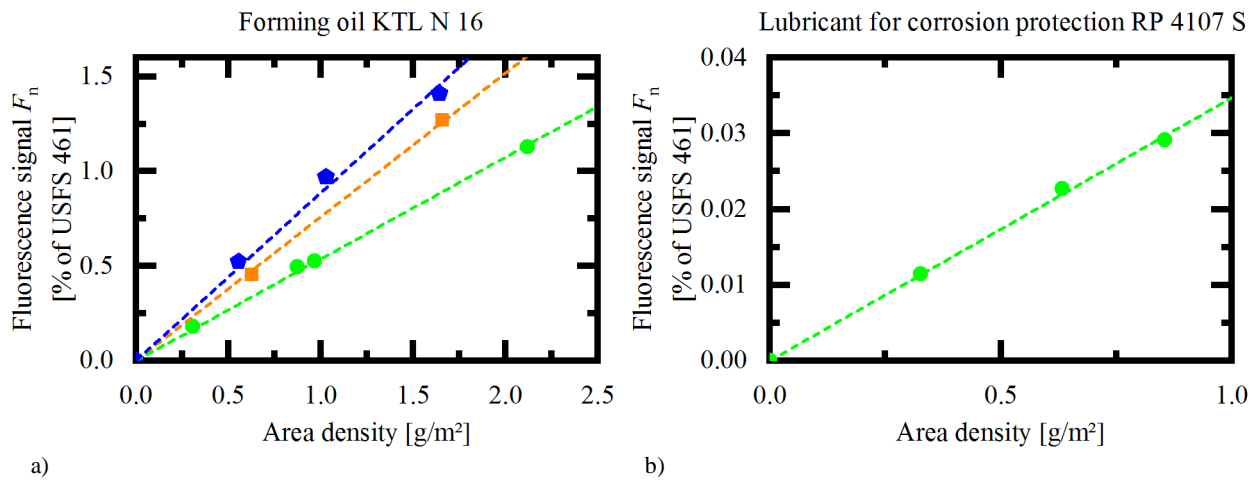


Figure 7. Calibration of the lab system for the forming oil KTL N 16 (a) as well as the lubricant for corrosion protection RP 4107 S (b). KTL N 16 was applied by rolling on pretex textured steel (●), EDT textured aluminum (■) and EDT textured steel (●), RP 4107 S only to EDT textured steel. As reference to the fluorescence signal, the applied lubricant layers were weighted using a high-resolution balance. All fluorescence signals are normalized to the emission of the reference target USFS-461.

These results show that both the surface type as well as the lubricant type influence the fluorescence signal emitted per layer thickness. Based on this results further work is necessary to understand all effects influencing the fluorescence response of lubricants on metal surfaces.

3.2 Calibration by multiphase carbon analyzer for thin layers

The application of 1.3 mg of lubricant on a sample with the size of 80 x 80 mm² leads to an area density of 0.2 g/m². Therefore, for lower area densities of lubricant the precession of precession balances is not sufficient to determine the average thickness of thin lubricant layers. As described in section 2.4 we use a multiphase carbon analyzer to indirectly determine the amount of lubricant on metal surfaces. Figure 8 shows the calibration of the lab system for a rolling oil applied on copper samples. For the experiments leading to the results presented in Figure 8 the lubricant layers were prepared by rolling.

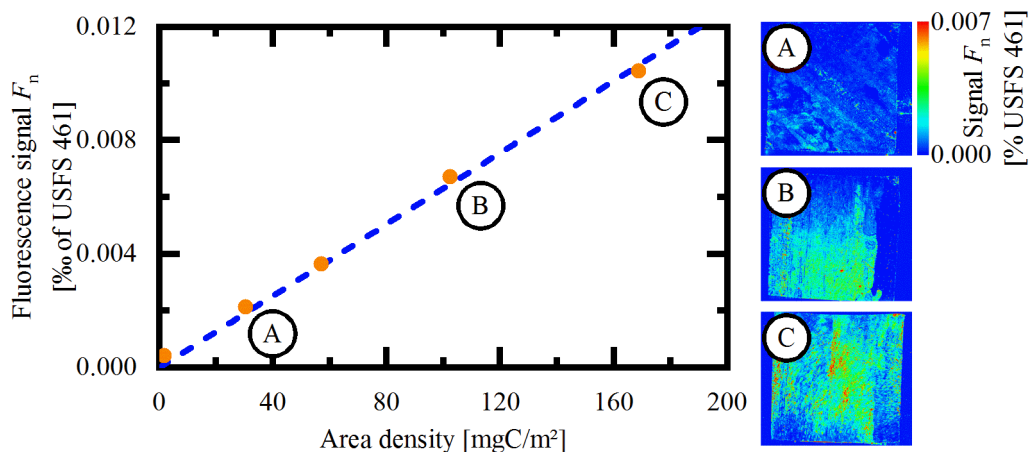


Figure 8. Calibration of the lab system for a rolling oil. As reference to the fluorescence signal the applied lubricant layers were characterized using a multiphase carbon analyzer. All fluorescence signals are normalized to the emission of the reference target USFS-461.

The blue line in Figure 8 visualizes the good linear relation between the detected fluorescence signal F_n and the total amount of carbon determined by the multiphase carbon analyzer, as expected in equation 4 and 6. This result clearly shows that a multiphase carbon analyzer can be used to calibrate the developed imaging fluorescence measurement systems. Based on these results the maximum error of quantification introduced by the presented lab setup is $\pm 5 \text{ mgC/m}^2$ for the calibrated rolling oil on copper. As shown in Figure 8 the limit of detection of the presented lab setup is better than 20 mgC/m^2 for the calibrated rolling oil on copper samples.

Further work has to be done to determine the relation between the amount of carbon on the surface detected by the multiphase carbon analyzer and the actual area density of lubricant.

3.3 Field of view

To determine the field of view of the newly developed scanner system we installed the optical unit on top of a forklift. The distance between the bottom of the housing and the samples surface was $l_{\perp} = 1.45$ meters. For the analysis of the field of view the same samples were analyzed at different positions within the field of view. We used a linear stage to move the sample through the area monitored by the laser scanner.

The fluorescence images shown in Figure 9 compare the raw data that is acquired, if the same samples are placed at different position within the field of view of the newly developed polygon scanner. The fluorescence images show EDT textured aluminum samples coated with the forming oil KTL N 16. The samples shown in Figure 9 are identical to the samples shown in Figure 6. Figure 6 shows high-resolution fluorescence images of these samples. In addition, the fluorescence image in Figure 9 shows the reference target suggested in section 2.3. This two inch fluorescent reference target USFS 461 is visible as the circular object placed right of the metal sample.

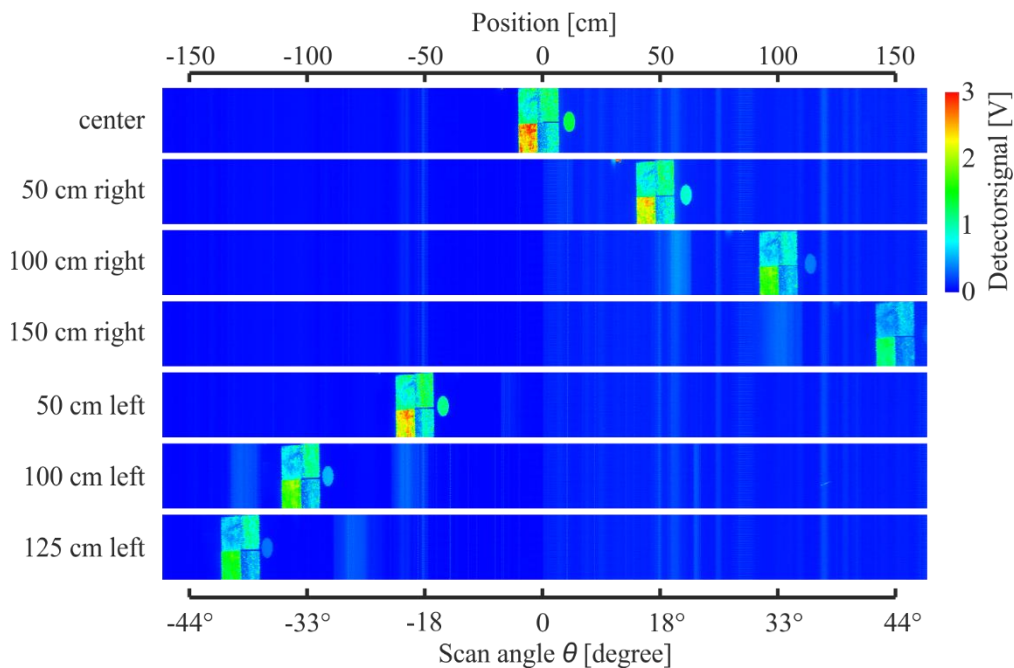


Figure 9. Analysis of the field of view of the newly developed fluorescence scanner. The fluorescence images show the raw data that is acquired, if the same samples are placed at different position within the field of view. If the housing is installed at height of $l_{\perp} = 145 \text{ cm}$ a field of view of 300 cm is reached.

As shown in Figure 9 the presented setup allows the analysis of sample in an angular field of 88° . In the exemplary installation made for the described experiment this leads to a field of view of up to three meters.

The comparison of the fluorescence images in Figure 9 visualizes the decrease of the detected fluorescence signal as function of the sample position. The plots in Figure 10 show the raw fluorescence signal as function of the scan angles θ . The diagrams show the results for closed lubricant layers (a) as well as lubricant droplets (b) coated on different metal

surfaces. In addition, the left plot (a) show the raw fluorescence signal, if the suggested fluorescence standard is analyzed at different scan angles.

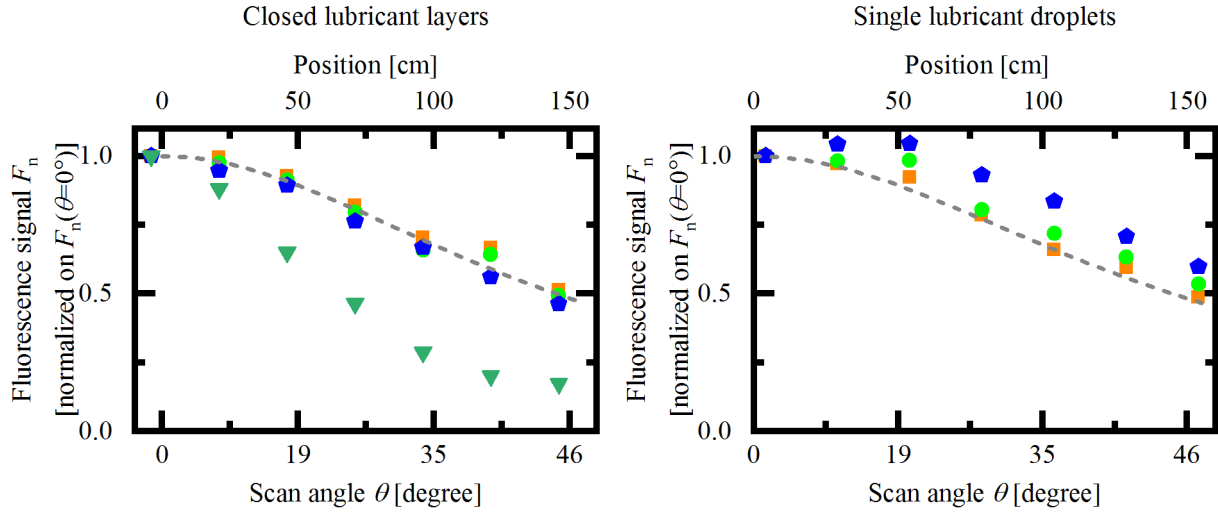


Figure 10. Raw fluorescence signal as function of the scan angle θ . The plots show the results for closed lubricant layers (a) as well as lubricant droplets (b) coated on different metal surfaces. For this experiment the forming oil KTL N 16 was coated on pretex textured steel (◆), EDT textured aluminum (■) and EDT textured Steel (●). In addition, the left plot (a) shows the results for analyzing the suggested reference target USFS 461 (▼) at different scan angles θ . The dashed line (—) indicates the reciprocal value of the square of the distance l between detector aperture and sample surface.

Figure 10a shows that the decrease of the raw fluorescence signal as function of the scan angle is independent of the surface textured for closed lubricant layers. According to equation 5 the detected fluorescence signal decreases reciprocal to the square of the distance l between detector aperture and sample surface. The dashed line indicates the square of the distance $l(\theta)$ as a function of the scan angle θ normalized to the minimal distance l_1 . The experimental results plotted in Figure 10a show a good correlation with the theory described by equation 5.

Figure 10b shows the experimental results for lubricant droplets coated on different textured metal samples. The results indicate as well a good correlation between the signal decreases described by equation 5 and the signals detected for lubricant droplets on steel and aluminum samples with EDT textured surfaces.

The results for lubricant droplets coated on pretex textured steel deviate from the signal decreases described by equation 5. As displayed in the microscope images in Figure 5 the so-called pretex surface consists of many hemispherical cavities. Ray tracing simulations by Fraunhofer IPM on this effect suggest that some portion of the excitation light is guided inside the lubricant droplets. The amount of excitation light coupling into the lubricant droplets depends on both the contact angle of the droplets as well as the illumination angle θ . The increase of the optical path length d , caused by multiple reflections inside the droplets leads to an increasing fluorescence response as function of the illumination angle θ .

The results for the fluorescent reference target USFS 461 suggested in section 2.3 as well deviate from the signal decreases described by equation 5. This deviation has to be considered if this reference target is used for the comparison of fluorescence signals detected by different optical setups as described in section 2.3. One possible reason for this effect could be a directed emission characteristic of the fluorescence light due to the sample structure.

3.4 In-line integration

The properties of the newly developed in-line measurement system presented in this paper, enables the implementation of completely new industrial applications. One novel application is the controlled lubrication of sheet metal blanks based on the individual pre-lubrication of each blank. This application was never implemented before, due to the lack of in-line measurement systems fulfilling the requirements on spatial resolution for this application.

To realize a controlled lubrication system, the in-line measurement system presented in this paper was permanently installed on a spray lubrication system developed by Raziol® Zibulla & Sohn GmbH. Figure 11 shows the final system, consisting of a belt system to transport metal blanks, the measurement system (A) as well as the actual spray chamber (B). The spray lubrication system shown in Figure 11 allows the lubrication of metal sheets with a width of up to one meter. The total number of 20 spray heads allows the generation of lubricant patterns with a spatial resolution of 5 x 5 cm². In contrast to the scanner-system described in section 2.2, the optical unit, shown in Figure 11, contains only one channel. Therefore, the angular field is reduced to 60°, which is sufficient for this application.

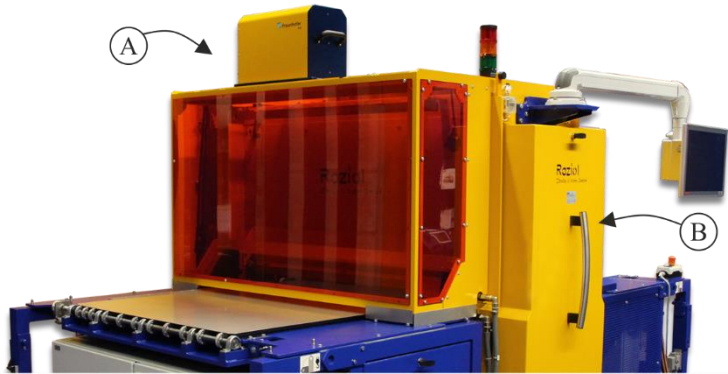


Figure 11. Spray lubrication system (B) developed by Raziol® Zibulla & Sohn GmbH equipped with the presented novel in-line measurement system (A). Combining the high-resolution measurement system with the spatial resolved lubrication unit allows the controlled generation of lubricant patterns based on the individual pre-lubrication of each blank.

As shown in Figure 11, we enclose the scan area with laser safety windows. By using these windows, the complete system is classified as class 1 laser system and can thus be used outside any lab environment. Furthermore, the laser safety windows suppress ambient light in the wavelength range from 400 to 520 nm. Ambient light in this spectral range would interfere with the fluorescence emission of typical lubricants. Figure 12 shows the flowchart of the implemented controlled lubrication system.

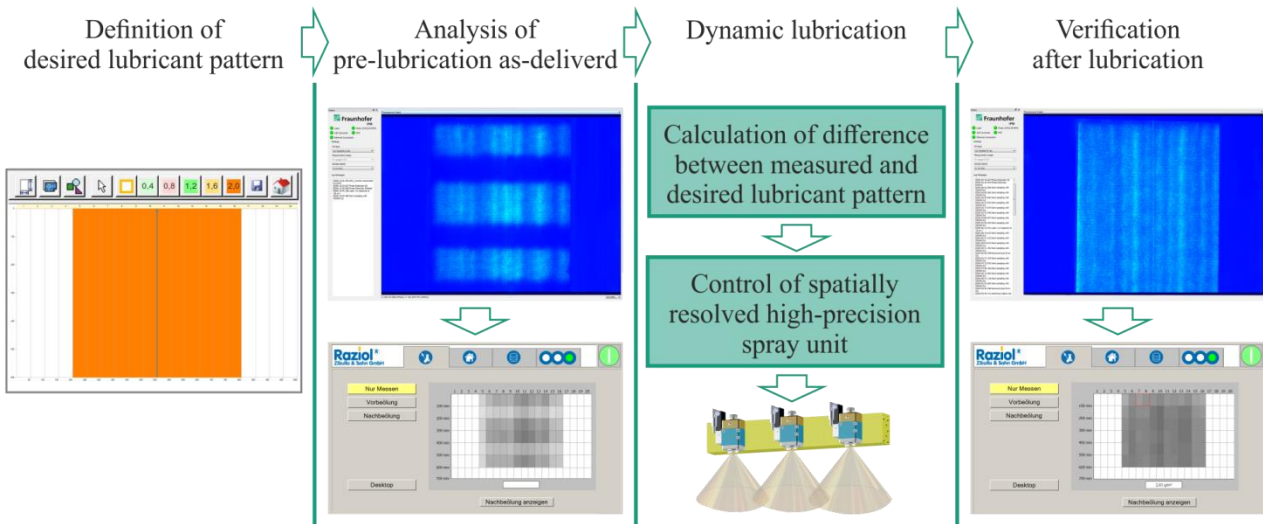


Figure 12. Flowchart of the implemented controlled lubrication system. The software calculates the difference between the desired lubricant pattern and the lubricant distribution detected by the presented measurement setup. Based on this computation the spray unit dynamically lubricates each metal blank with an individual pattern to produce the desired lubricant distribution.

Initially the user defines the desired lubricant pattern in the graphical user interface of the software of the lubrication system. After inserting, the belt system is moving the pre-lubricated metal blank through the field of view of the laser scanner. The software of the laser scanner uses the high-resolution fluorescence image to calculate the lubricant

distribution in the spatial resolution defined by the spray heads. This fluorescence image is transferred to the software of the lubrication system. Based on this information, the software determines the difference between the desired lubricant pattern and the lubricant distribution detected by the presented measurement setup. This dynamically calculated lubrication pattern is then transferred to the control electronics of the spray heads. Finally, the belt system moves the metal blank through spray chamber to apply the lubricant. Optionally the final lubricant distribution can be validated by a second fluorescence measurement.

Experimental results of the automated completion of a desired lubricant pattern based on fluorescence images acquired by the presented system are shown in the screenshots used in the flowchart in Figure 12. Therefore, the presented lubrication system ensures the presence of a desired lubricant pattern independently of varying pre-lubrications on different metal sheets.

The implemented system combines for the first time an imaging system for lubricant thickness measurements with a controlled lubrication unit. This novel tool enables advanced experiments in the field of tribology as well as metal forming.

4. CONCLUSION

We have presented a new optical setup that is capable to monitor the spatial distribution of functional coatings on metal surfaces moving on production speeds up to several meters per second.

The setup uses a rotating polygon-scanning mirror to deflect a laser beam on the sample surface. During the scan, the excitation laser induces fluorescence locally on the probe. As the sample moves perpendicular to the scan-axis, the setup allows the acquisition of two-dimensional images of e.g. lubricant distributions. The angular field of the presented system is 88° . Therefore, installing the scanner system at a distance of 1.2 m above the probe, realizes a field of view of 2.2 m.

For the calibration of the system, samples were prepared using a rubber roll as well as a spray system. We have presented two reference methods for the characterization of the prepared lubricant layers. For lubricant layers in the range of 0.2 to 2.5 g/m² we used a high-resolution balance as reference. For lubricant layers in the range of 0.02 to 0.5 g/m² we used multiphase carbon analyzer as reference. The experimental result show that both the texture of the sample surface as well as the lubricant type influence the fluorescence signal emitted per layer thickness.

Based on this results further work is necessary to understand all effects influencing the fluorescence response of lubricants on metal surfaces. The results of simulations as well as more detailed experiments on this topic will be published in a separate publication.

For proof of concept, we integrated the novel measurement setup into a commercial spray oiler. This combination allows for the first time the controlled lubrication of sheet metal blanks based on the individual pre-lubrication of each blank. The presented lubrication system automatically ensures the presence of a desired lubricant pattern, independently of varying pre-lubrications on different metal sheets.

ACKNOWLEDGMENTS

The systems presented in this publication were developed in the group Optical Surface Analytics at Fraunhofer IPM. We thank Stefan Adolph for the mechanical engineering, Jens Scherer for the electrical engineering and Christian Lutz for the software engineering.

We thank Raziol® Zibulla & Sohn GmbH for providing pictures and screenshots of their spray lubrication system equipped with our fluorescence laser scanner. Whereas we provided the measurement system, Raziol® Zibulla & Sohn GmbH finally implementation the presented combined system for the controlled lubrication of sheet metal blanks based on the individual pre-lubrication of each blank.

The research leading to these results has received funding from the German Federal Ministry for Economic Affairs and Energy (Central Innovation Programme for SMEs (ZIM), Grant# ZF4036504 PO6)

REFERENCES

- [1] Purr, S., Wendt, A., Meinhardt, J., Moelzl, K., Werner, A., Hagenah, H. and Merklein, M., “Data-driven inline optimization of the manufacturing process of car body parts,” *IOP Conf. Ser. Mater. Sci. Eng.* **159**(1), 012002 (2016).
- [2] Van Stein, B., Van Leeuwen, M., Wang, H., Purr, S., Kreissl, S., Meinhardt, J. and Back, T., “Towards Data Driven Process Control in Manufacturing Car Body Parts,” *2016 Int. Conf. Comput. Sci. Comput. Intell.*, 459–462, IEEE (2016).
- [3] Singh, C. P. and Agnihotri, G., “Study of Deep Drawing Process Parameters : A Review,” *Int. J. Sci. Res. Publ.* **5**(2) (2015).
- [4] Purr, S., Meinhardt, J., Lipp, A., Werner, A., Ostermair, M. and Glück, B., “Stamping Plant 4.0 – Basics for the Application of Data Mining Methods in Manufacturing Car Body Parts,” *Key Eng. Mater.* **639**, 21–30 (2015).
- [5] Bilstein, W., Enderle, W., Moreas, G., Oppermann, D., Routschek, T. and Van De Velde, F., “Two systems for on-line oil film and surface roughness measurement for strip steel production,” *Rev. Métallurgie* **104**(7–8), 348–353 (2007).
- [6] Matthias, I., Aha, B. and Zimmermann, R., “EMG – Online-Qualitätssicherung für den Abpressprozess: Festigkeit, Rauheit und Ölaufgabe in Kombination,” *Prozesstechnik der Blechverarbeitung - Interaktion Maschine | Werkzeug*, 105–125, Europäische Forschungsgesellschaft für Blechverarbeitung (Hg.) (2016).
- [7] Bley, H. and Oberhausen, M., “Metrological approaches for meeting the requirements of clean production,” *Toward. a Closed Loop Econ. 13th CIRP Int. Conf. Life Cycle Eng.*, 619–622 (2006).
- [8] Schreiner, C., “EMG SOLID® IR and LIF: Two systems, one DNA,” <<http://www.emg-automation.com/en/details/emg-solidr-ir-und-lif-zwei-systeme-eine-dna/>> (10 April 2017).
- [9] Morton, C. E., Baker, R. C. and Hutchings, I. M., “Measurement of liquid film thickness by optical fluorescence and its application to an oscillating piston positive displacement flowmeter,” *Meas. Sci. Technol.* **22**(12), 125403 (2011).
- [10] Wigger, S., Füßer, H.-J., Fuhrmann, D., Schulz, C. and Kaiser, S. A., “Quantitative two-dimensional measurement of oil-film thickness by laser-induced fluorescence in a piston-ring model experiment,” *Appl. Opt.* **55**(2), 269 (2016).
- [11] Hengstermann, T. and Reuter, R., “Laser Remote Sensing of Pollution of the Sea: a Quantitative Approach,” *EARSeL Adv. Remote Sens.* **1**(2–II), 52–60 (1992).
- [12] Hengstermann, T. and Reuter, R., “Lidar fluorosensing of mineral oil spills on the sea surface,” *Appl. Opt.* **29**(22), 3218–3227 (1990).
- [13] Holz, P., Lutz, C. and Brandenburg, A., “Optical scanner system for high resolution measurement of lubricant distributions on metal strips based on laser induced fluorescence,” *Proc. SPIE 10329, Opt. Meas. Syst. Ind. Insp. X*, P. Lehmann, W. Osten, and A. Albertazzi Gonçalves, Eds., 103292A, SPIE (2017).
- [14] Valeur, B., [Molecular Fluorescence], Wiley-VCH Verlag GmbH, Weinheim, FRG (2001).
- [15] Labsphere Inc., “Datasheet Spectralon Diffuse Fluorescence Materials,” 2015, <<http://labsphere.com/labsphere-products-solutions/materials-coatings-2/coatings-materials/fluorescence-materials/>> (10 April 2017).
- [16] Zhou, R., Cao, J., Wang, Q. J., Meng, F., Zimowski, K. and Xia, Z. C., “Effect of EDT surface texturing on tribological behavior of aluminum sheet,” *J. Mater. Process. Technol.* **211**(10), 1643–1649 (2011).
- [17] Heidelberger, F., “Electrolytically galvanized steel grades,” *Prod. Mag. Sal-Z*(7), 20 (2014).
- [18] Leco Corporation., “Application Note: Surface Carbon on Steel Sheet and Rod Samples,” 3 (2008).